



## THEORETICAL STUDIES OF DYNAMIC SOIL COMPACTION BY WHEELED FORESTRY MACHINES

**Igor GRIGOREV<sup>1</sup>, Olga KUNICKAYA<sup>1</sup>, Albert BURGONUTDINOV<sup>2</sup>, Viktor IVANOV<sup>3</sup>,  
Svetlana SHUVALOVA<sup>4</sup>, Viktoria SHVETSOVA<sup>4</sup>, Marina STEPANISHCHEVA<sup>5</sup>,  
Evgeniy TIKHONOV<sup>6</sup>**

<sup>1</sup> Department of Technology and Equipment of Forest Complex, Yakut State Agricultural Academy, Yakutsk, Russian Federation. [grigorevig11@rambler.ru](mailto:grigorevig11@rambler.ru)

<sup>2</sup> Department of Roads and Bridges Building, Perm National Research Polytechnic University, Perm, Russian Federation

<sup>3</sup> Bratsk State University, Bratsk, Russian Federation

<sup>4</sup> Department of Descriptive Geometry and Engineering Graphics, Saint Petersburg State University of Architecture and Civil Engineering, Saint-Petersburg, Russian Federation

<sup>5</sup> Department of Reproduction and Processing of Forest Resources, Bratsk State University, Bratsk, Russian Federation

<sup>6</sup> Department of Transport and Technological Machinery and Equipment, Federal State Budget Educational Institution of Higher Education "Petrozavodsk State University", Petrozavodsk, Russian Federation

### Abstract

The impact of forest skidding machine tires on the soil differs depending on topography, soil properties, and type of the wheel system. The development of a mathematical model describing the entire dynamic process is a challenging but relevant task to assess the level of impact. The work aims mathematical modeling of the impact caused by the skidding system on the forest soil employing Kelvin-Voigt theory with additional elastic element and Laplace transform equations. A dynamic model represents the "tractor-timber bundle-soil" system. According to the results of mathematical modeling, it was found that studying the vertical vibrations and vibrations of sprung mass in longitudinal and transverse planes is sufficient for examining dynamic soil compaction. Developed methods of statistical dynamics with the presentation of the track surface microroughness and the theory of linear elastic and viscous soil deformation showed that each pass of the skidding system is accompanied by additional dynamic soil compaction. Its maximum value depends on the properties of the soil and skidding system, as well as on the presence of resonant zones in the frequency spectrum. The results of these studies provide an opportunity to predict the exposure level of skidders and establish new solutions to minimize negative consequences for the environment and productivity of the forest industry.

Keywords: D'Alembert's principle; dynamic soil compaction; Laplace transform; tractor's cyclic circuit; the Kelvin-Voigt model

## 1. INTRODUCTION

When developing the timber harvesting technologies in forests, it is necessary to consider various factors such as soil composition, the level of impact of harvesting machines and their technological aspects on the soil, as well as natural and climatic conditions. Forest harvesting operations cause a significant negative impact on the soil leading to its wounding by skidders, compaction, and rutting.

The results of experimental studies show varying degrees of skidding machinery impact on the soil degradation due to reduced water penetration, which increases the risk of soil erosion [1-3]. The compaction and deformation of the soil occurring during the passage of forest machinery are considered as complex processes that depend on

the pressure, shear forces, and spread of vibrations in the soil. According to a literature review [24], these negative effects can affect the soil to a depth of 0.75 m. Moreover, the soil can recover only within 1-2 years after the first passage of the machine unless no further impacts are exerted. Subsequent passages of the machines induce additional compaction. Such negative impacts on the soil lead to limited moisture and nutrients content required for plant seeds and result, eventually, in changing forest ecosystems in such areas [25].

The authors in [26] examined samples of disturbed and undisturbed soil at different depths to determine the physical parameters of the soil and reported that soil compaction is characterized by such methods as elastic deformation, plastic

deformation, disturbance of bearing capacity, and homogenization of soil structure.

In this regard, the theoretical study of dynamic soil compaction by forest machinery is highly relevant. For example, the paper [27] suggests the method for measuring the dynamic pressure on the soil by given parameters of the weight and speed of the forest machine based on theoretical experimental data. Theoretical studies of dynamic soil compaction by wheeled forest machines and skidding systems based on it *are performed from simple (4x4) to complex (8x8) tractor modification*. As the skidding system is an extremely complex vibrating system involving a large number of discrete and distributed masses, the dynamic system is more complicated due to the elastic and viscous properties of soil. To simplify the process, an equivalent vibrating system or analytical reduced scheme equivalent to a dynamic system [4] was accepted to study and estimate oscillations in a certain frequency range.

Equivalent cyclic circuit of a skidding system, as well as the majority of real dynamic and physical systems, is nonlinear [4] at an exact estimation but experimental studies of lorries [5] and wheeled skidders [6] have shown that elastic characteristics of tires and suspension in a deformation zone near static loading are close to linear. The analysis of skidding systems based on the wheeled tractor has shown that masses and their moments of inertia in a particular system are set and constant, and the equivalent scheme should be considered as a vibrational system with constant dynamic parameters [7].

When investigating the machine's vibrations in equivalent vibrating schemes, the pneumatic tire is depicted as a spring on the wheel axle, the lower end of which moves on the supporting surface. Calculations according to the developed mathematical models in [8] have shown that the flattening of the road microprofile of the automobile proving ground is much more intensive at fine roughness rather than at long. For our research, the examination of the flattening effect of the field surface microroughness of the machine-tractor unit with a soil tillage machine is of high interest [9]. Microroughness can be flattened under the influence of supporting wheels, while others are copied by wheels. Normal correlation functions and spectral densities of unevennesses after each passage are identical. Therefore, in calculations for investigating the dynamics of soil tillage machines, statistical characteristics of surface unevennesses received before the passage of the machine are applied. The latest studies on wheeled vehicle vibrations and elastic properties of the soil show that their behavior is evaluated by different physical and mechanical parameters [13-17]. It confirms the relevance of examining each of the two subsystems separately. Vibrations of the first subsystem under the influence of disturbances from the trail

microroughness contribute to additional dynamic compaction of the soil.

The purpose of this work was to study the dynamic compaction of the soil by wheeled forestry machines presented as a dynamic model of the system "tractor – timber bundle - soil", which consists of two systems: the vibration of a tractor and tractor with a bunch of wood on tires. The results of these studies provide an opportunity to predict the exposure level of skidders and establish new solutions for minimization of negative consequences for the environment and productivity of the forest industry.

## 2. MATERIALS AND METHODS

Theoretical studies include studying the vibrations of tractors with 4x4, 6x6, and 8x8 wheel modifications produced by numerous leading manufacturers of forest machinery such as John Deere, Ponce, Komatsu, Rottne, etc. [10]. The structural feature of forest wheeled tractors is that the relative turn of the rear and front half-frame in the transverse plane is accompanied by a twisting of the cardan drive. At that, the rigidity of the half-frame is considered to be higher than that of the cardan drive. Fig. 1 shows the oscillating scheme of the system equivalent to the vibrations of tractors with 4x4 wheels.

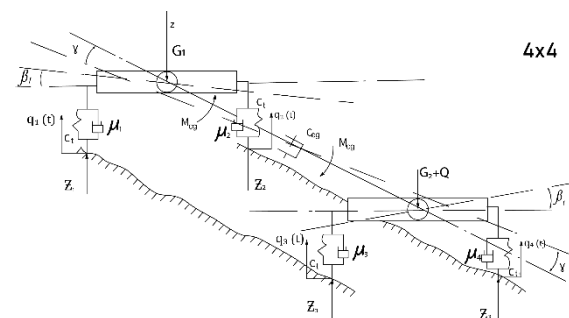


Fig. 1. Oscillating scheme of the tractor with 4x4 wheel arrangement.  $G=G_1+G_2$  is the weight of the tractor;  $G_1$  and  $G_2$  is the weight of the rear and front half-frames, respectively;  $Q$  is the weight of timber bundle;  $Q_1$  is the weight of the bundle placed on the tractor;  $C_t$  is the coefficient of tire rigidity;  $\mu_t$  is the coefficient of viscous friction of the tire;  $\beta_f$  and  $\beta_r$  are the turning angles of half-frames in the transverse plane, respectively;  $C_{CG}$  is the rigidity coefficient of the cardan gear;  $\gamma$  is the turning angle of half-frame in the longitudinal plane;  $M_{CG}$  is the torsion torque of the cardan gear;  $q_i$  is the coordinates;  $z_i$  is the soil reaction.

Dynamic soil compaction by the wheeled forestry machines, in special by a skidding system, can be represented by a dynamic model of the "tractor - timber bundle - soil" system consisting of two systems, one of which is the oscillation of a tractor or a tractor with a wood bunch on tires.

**Parameters of the oscillating system "skidding tractor - timber bundle"**

When simplifying and compiling the above calculation schemes, which are equivalent to an oscillating or dynamic system, the distributed mass of a skidding tractor with a bundle of wood are replaced by discrete mass connected by elastic non-inertial bonds and reflecting the rigidity or pliability of the elastic elements inclusive of coupling friction and intramolecular friction in the tire. To comprise a simplified scheme of the equivalent "skidding tractor - timber bundle" oscillating system, it is necessary to justify and select the dynamic parameters of the vibrating system.

Under the influence of unevenness of the harvesting area supporting surface, first of all of the skidding trail, the skidding system performs vertical and angular oscillations in longitudinal and transverse planes. The degree of complexity of the equivalent oscillating scheme of the skidding system is determined by the number of structural elements included in the consideration, elastic and damping properties, and the nature of the disturbing influences.

The masses and moments of inertia of the oscillating system are mainly determined by the masses of the front and rear half-frames with the units, mechanisms, systems, equipment, and wood placed on them. The oscillating system in advanced forest machinery is characterized by the absence of springs and shock absorbers. Its functions are performed by large-sized forest tires, which can be referred to as extra-low pressure tires according to common tire classification.

The inertia moments of the wheeled tractors and their half-frames in transverse and longitudinal planes is not possible to determine experimentally. When studying the oscillating system equivalent to the running gear of a lorry, the distribution of sprung masses in the longitudinal plane is determined, which is characterized by the index of vertical vibrations inertia over the front and rear suspension  $\varepsilon$ , in our case, over the axles and trolleys. Thus, it follows:

$$\varepsilon = \frac{\rho_m^2}{a \cdot b}, \tag{1}$$

where  $\rho_m$  is the radius of the sprung mass inertia in relation to the transverse axis passing through the center of gravity, and  $a, b$  is the distance from the center of the sprung mass to the front and rear axles (to the trolley axle in balance trolley) along the longitudinal axis of the machine.

Complex configuration of the tractor with a timber bundle and its half-frames complicates the determining with high precision the moments and radii of inertia. In theoretical mechanics [12], the formulas for determining the inertia moments and radii of homogeneous bodies with different shapes are proposed, which can be used for similar calculations in our research. The torque of a

rectangular parallelepiped with respect to the axis of symmetry (x) is equal:

$$J_x = M \frac{a_T^2 + b_T^2}{12} \tag{2}$$

and the radius of inertia amounts to:

$$\rho_x = \frac{\sqrt{a_T^2 + b_T^2}}{2\sqrt{3}} = 0,289\sqrt{a_T^2 + b_T^2} \tag{3}$$

where  $a_T$  and  $b_T$  is the width and height of the parallelepiped in relation to the x axis, respectively.

Tire rigidity manifests at all investigated vibrations: vertical, transverse, and longitudinal angular. Researchers of lorries with high loading capacity have established linear dependence of elasticity of front (tires and shock absorbers) and rear (only tires) suspensions, especially within the range of real deformations and air pressure in the tire recommended by manufacturers [13, 28].

Oscillations of the skidding system in the transverse plane are accompanied by angular movements of the front and rear half-frames to a relative twist angle. Its maximum value for a wheeled forest tractor can reach 17° (Fig. 2). In this case, the cardan gear transmitting the torque from the transfer gearbox to the rear axle also twists. [14] The stiffness coefficient for cardan gear equals to  $5,1 \cdot 10^4$  H·m/rad. The half-frames of the articulated frame are connected by a joint to a plane bearing in which friction is negligible.

In equivalent oscillating schemes of skidding systems based on wheeled tractors, the coefficients of radial stiffness and inelastic resistance of tires for each axle should be considered as parallel included elements. Their values for each axle are summed up [15]. Table 1 shows the coefficients of radial stiffness and inelastic resistance for single tires and tires of one trolley side, i.e., two tires.

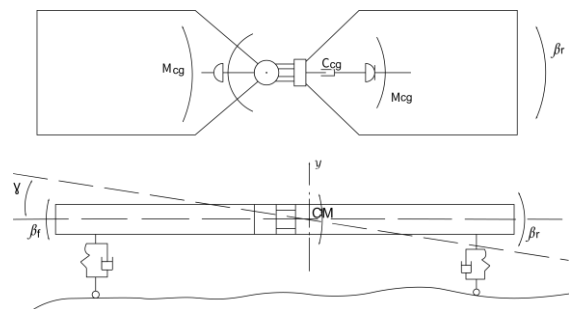


Fig. 2. The scheme of hinge twisting

Table 1. Coefficients of radial stiffness and inelastic resistance of tires

Parameters	Size	Values			
		Tire 33L-32	Tire 23,1-26	Two tires 23,1-26 of the trolley or axle	Two tires 33L- of the trolley or axle
<b>Stiffness coefficient</b>	kN/m	1300	900	1800	2600
<b>Coefficients of inelastic resistance</b>	kN·s/m	20,0	12,0	24	40

### Equivalent scheme of the dynamic system "tractor-timber bundle-soil"

When studying the dynamic compaction of the soil by the skidding system under the disturbing effects of microroughness of the track surface, the dynamic system "tractor-timber bundle-soil" is accepted to be divided into two subsystems [16]. The first subsystem reflects the oscillations of the skidding system on elastic tires in a radial direction and the second - elastic deformation of the soil under the dynamic influence of the skidding system [17].

Similarly to the terms used in the studying lorries, the first subsystem of the dynamic system "tractor-timber bundle-soil" can be referred to as a scheme of the oscillating subsystem, equivalent to the vibrations of a tractor or tractor with a bunch of wood on the tires [17]. Such schemes of oscillating systems based on tractors with 4x4 wheel configurations are given in Fig. 3.

Wheeled skidders with a 4x4 wheel configuration are usually equipped with a pincer grab. The connection scheme of a semi-suspended bunch of wood is shown in Fig. 4a.

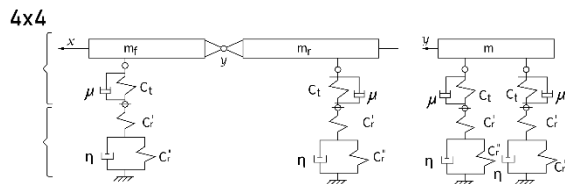


Fig. 3. Oscillating systems based on tractors with various wheel configurations,  $M$  is a tractor weight with wood,  $m_f$  and  $m_r$  are the weights of front and rear half-frames, respectively,  $c_s'$ ,  $c_s''$  is the soil parameter, and  $\eta$  is the soil viscosity coefficient.

On a chokerless wheeled tractor with hydraulic grapple of the tree butts, the bundles of wood are placed into clam bunk. The scheme of connection between the semi-suspended bunch of wood with the tractor is shown in Fig. 4b.

When investigating the first subsystem, the influence of vertical oscillations and oscillations in longitudinal and transverse planes on dynamic soil compaction was studied. Calculations have shown that the first natural frequency of vertical oscillations of the skidding system is a little higher than the first natural frequency of trees transverse oscillations and varies within the range of 0.6-0.7 Hz [18]. Besides, the mass of wood bundle leaning on the soil is about 10% of the skidding system mass based on TLK 4-01 tractor. Consequently, vertical oscillations of the skidding system can be investigated separately from the transverse vibrations of the timber bundle.

Also, the following assumptions have been made for an equivalent calculation scheme:

- angular oscillations occur around the roll and trim axes;
- tire deformation is unlimited;

- vertical oscillations do not affect angular oscillations [19];
- the relative rotation angle of the half-frames is no more than  $17^\circ$ .

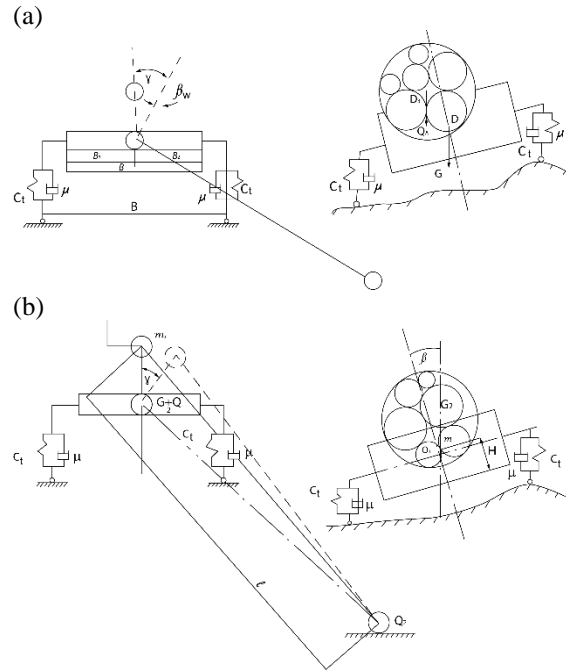


Fig. 4. (a) – the connection scheme for a semi-suspended bundle of wood,  $\gamma$  is the deviation angle of suspension;  $\beta_w$  is the angle of deviation of wood bundle; (b) - scheme of connection between a semi-suspended bundle of wood with a tractor.

When investigating the first subsystem, the influence of vertical oscillations and oscillations in longitudinal and transverse planes on dynamic soil compaction was studied. Calculations have shown that the first natural frequency of vertical oscillations of the skidding system is a little higher than the first natural frequency of trees transverse oscillations and varies within the range of 0.6-0.7 Hz [18]. Besides, the mass of wood bundle leaning on the soil is about 10% of the skidding system mass based on TLK 4-01 tractor. Consequently, vertical oscillations of the skidding system can be investigated separately from the transverse vibrations of the timber bundle.

Also, the following assumptions have been made for an equivalent calculation scheme:

- angular oscillations occur around the roll and trim axes;
- tire deformation is unlimited;
- vertical oscillations do not affect angular oscillations [19];
- the relative rotation angle of the half-frames is no more than  $17^\circ$ .

### 3. RESULTS AND DISCUSSION

#### First subsystem

The oscillating process of the skidding system at passage through a logging area is determined not only by the disturbing effects of the trail, but also by the properties of the dynamic system, which in our research is a skidding tractor or skidding system, i.e., tractor with a bundle of wood on the tires.

Tractor or a skidding system can perform following oscillating movements: linear, longitudinal, transverse, etc. Only the sprung weight of the tractor in space can have six degrees of freedom, that is, its movement can be determined by three linear and three angular coordinates. In modern wheeled forest tractors such technical and design solutions are used, which provide a straight-line motion, that is, excluding longitudinal linear oscillations and "yawing", at which the movement of the machine can be uncontrollable [16].

Considering the vibrations of the tractor on tires and taking into account the vibrations of semi-loaded or semi-suspended timber bundle, as well as transmission and engine vibrations, the number of freedom degrees increases. In our research, the vibrations of the tractor and the skidding system on tires are investigated not considering the torsional vibrations of the transmission and engine.

Consequently, the vibrations of a tractor and a tractor with a fully loaded bundle of wood can be considered as a dynamic oscillating system with four degrees of freedom (Fig. 1). The first degree of freedom is vertical vibrations of the tractor on tires together with the center of mass,  $Z$  coordinate. The second degree of freedom is the longitudinal angular oscillations, the turning of tractor mass with the loaded wood relative to the center of mass or its transverse coordinate. At such oscillations position of the sprung mass of the system relative to the center of mass is determined by coordinate  $\beta$ .

The third degree of freedom is the transverse angular oscillations of the two hinged half-frames. At that, the position of the front and rear half-frames relative to the center of mass or its longitudinal coordinate  $x$  is determined by  $\gamma$ . The oscillations of the front half-frame relative to the rear half-frame and vice versa are the fourth degree of freedom. In addition to the hinged connection with relatively low friction moment value, the half-frame is connected by a cardan gear with the rigidity coefficient  $C_c$ .

Sprung systems of all wheeled forest tractors are symmetrical with respect to the longitudinal axle of the machine [13, 16]. Longitudinal angular oscillations of the sprung mass symmetrical with respect to machine longitudinal axle can be considered independently from transverse angular oscillations and vice versa.

The microprofile of the reference surface microroughness is usually represented by the

correlation function of action  $R(\tau_i)$ , which can be approximated as follows:

$$R(\tau_i) = D e^{-\alpha|\tau_i|} \cos \beta \tau_i \quad (4)$$

where  $D$  is the dispersion of microroughness and  $\alpha, \beta$  are the coefficients of approximation.

Lag time  $\tau_i = t_i - t_{i-1}$  at passage of the  $i$ -wheel of the machine on the unevenness compared to the passage of the first wheel:

$$\tau_i = \frac{l_i - l_1}{v} \quad (5)$$

where  $l_i$  is the distance of axles from the center of tractor mass and  $v$  is the tractor speed.

#### Forwarder or tractor without wood

The dynamic oscillation system of the skidding tractor is a holonomy system with constant parameters. The motion of the system will be considered in the inertial coordinate system connected with the ground. The equation of motion is composed as an equilibrium of acting forces applying D'Alembert's principle.

Differential equations of the system's motion (Fig. 5) can be presented as:

$$\begin{aligned} Z + a_1 Z + a_2 Z &= \frac{1}{M} (\sum_{i=1}^{2n} \mu_t y_i + \sum_{i=1}^{2n} C_t y_i) \\ \varphi + b_1 \varphi + b_2 \varphi &= \frac{1}{J_{lt}} (\sum_{i=1}^{2n} \mu_t l_i y_i + \sum_{i=1}^{2n} C_t l_i y_i) \\ \gamma_1 + C_1 \gamma_1 + C_2 \gamma_1 + C_{\gamma_1} (1 - \Delta \gamma) &= \\ \frac{1}{J_{lt}} (\sum_{i=1}^{2n} \mu_t l_i y_i + \sum_{i=1}^{2n} C_t l_i y_i) & \\ \gamma_2 + d_1 \gamma_2 + d_2 \gamma_2 + C_{\gamma_2} (1 - \Delta \gamma) &= \\ \frac{1}{J_{rt}} (\sum_{i=1}^{2n} \mu_t l_i y_i + \sum_{i=1}^{2n} C_t l_i y_i) & \end{aligned} \quad (6)$$

$$\begin{aligned} \text{where } a_1 &= \frac{2n\mu_t}{M}, \quad a_2 = \frac{2nC_t}{M}, \quad b_1 = \frac{\mu_t}{J_{lt}} \sum_{i=1}^{2n} l_i^2, \\ b_2 &= \frac{C_t}{J_{lt}} \sum_{i=1}^{2n} l_i^2, \quad C_1 = \frac{\mu_t}{J_{ft}} \sum_{i=1}^{2n} l_i^2, \quad C_2 = \frac{C_t}{J_{ft}} \sum_{i=1}^{2n} l_i^2, \\ d_1 &= \frac{\mu_t}{J_{rt}} \sum_{i=1}^{2n} l_i^2, \quad d_2 = \frac{C_t}{J_{rt}} \sum_{i=1}^{2n} l_i^2. \end{aligned}$$

$\Delta \gamma = \frac{\gamma_1 - \gamma_2}{\gamma_1}$  is the relative value of the half-frame angular deviation in an articulated joint and  $n$  is the number of axles of a multi-axle tractor,  $\mu_t$  is the coefficient of the tire viscous friction,  $C_t$  is the tire rigidity coefficient,  $M$  is a tractor weight with wood, torques of a rectangular parallelepiped relative to the axis of symmetry in longitudinal  $J_{lt}$ , as well as front  $J_{ft}$ , and rear  $J_{rt}$  transverse planes.

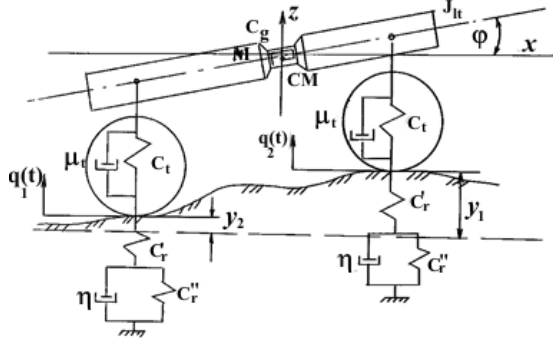
After Laplace transform of the differential equations system (6), a system of algebraic equations can look like:

$$\begin{aligned} (s^2 + a_1 s + a_2) z(s) &= \frac{1}{M} [F_1(s) \sum_{i=1}^{2n} (\mu_t s + C_t) e^{-\tau_i s}] \\ (s^2 + b_1 s + b_2) \varphi(s) &= \frac{1}{J_{lt}} [F_1(s) \sum_{i=1}^{2n} (\mu_t s + C_t) e^{-\tau_i s}] \\ (s^2 + c_1 s + c_2) \gamma_1(s) &= \frac{1}{J_{ft}} [F_1(s) \sum_{i=1}^{2n} (\mu_t s + C_t) e^{-\tau_i s}] \\ (s^2 + d_1 s + d_2) \gamma_2(s) &= \frac{1}{J_{rt}} [F_1(s) \sum_{i=1}^{2n} (\mu_t s + C_t) e^{-\tau_i s}] \\ F_1(s) &= L[f_1(t - \tau_i)] - L[y_i] \end{aligned} \quad (7)$$

where  $L$  is Laplace transform and  $s = \sigma + i\omega$  is complex frequency.

Thus, the Laplace transform allowed passing from the system of differential equations (6) of acting variable  $t$  to the system of algebraic equations (7) of complex variable  $s$ .

a)



b)

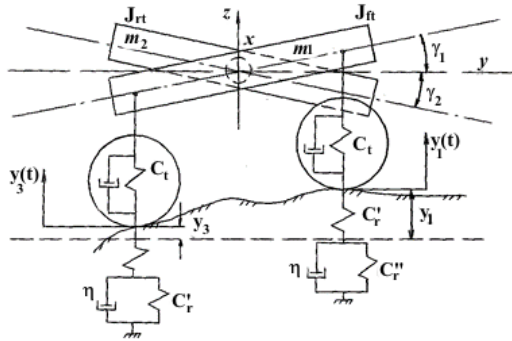


Fig. 5. Scheme of the oscillating system in the longitudinal (a) and transverse (b) plane equivalent to the skidding system.

By solving the system of questions (7) with the replacement of the determinant [11], the transfer functions of the reference surface to the sprung mass of the skidding system are determined  $W_z(s)$ ,  $W_\varphi(s)$ ,  $W_{y_1}(s)$ , and  $W_{y_2}(s)$  at the  $s=i\omega$  where  $\omega$  is the oscillation frequency,  $c^{-1}$ , and  $i$  is an imaginary unit. As a result, it follows:

$$W_z(i\omega) = \frac{K_\omega^z + iC_\omega^z}{M(M_\omega^z + iN_\omega^z)};$$

$$K_\omega^z = C_t \sum_{i=1}^{2n} l_i \cos \tau_i \omega + \mu_t \omega \sum_{i=1}^{2n} l_i \sin \tau_i \omega; \quad M_\omega^z = a_2 - \omega^2$$

$$C_\omega^z = \sum_{i=1}^{2n} l_i \cos \tau_i \omega - C_t \sum_{i=1}^{2n} l_i \sin \tau_i \omega; \quad N_\omega^z = a_1 \omega \quad (8)$$

$$W_\varphi(i\omega) = \frac{K_\omega^\varphi + iC_\omega^\varphi}{J_{lt}(M_\omega^\varphi + iN_\omega^\varphi)};$$

$$K_\omega^\varphi = C_t \sum_{i=1}^{2n} l_i \cos \tau_i \omega + \mu_t \omega \sum_{i=1}^{2n} l_i \sin \tau_i \omega; \quad M_\omega^\varphi = b_2 - \omega^2;$$

$$C_\omega^\varphi = \sum_{i=1}^{2n} l_i \cos \tau_i \omega - C_t \sum_{i=1}^{2n} l_i \sin \tau_i \omega; \quad N_\omega^\varphi = b_1 \omega \quad (9)$$

$$W_{y_1}(i\omega) = \frac{K_\omega^{y_1} + iC_\omega^{y_1}}{J_{ft}(M_\omega^{y_1} + iN_\omega^{y_1})};$$

$$K_\omega^{y_1} = C_t \sum_{i=1}^{2n} l_i \cos \tau_i \omega + \mu_t \omega \sum_{i=1}^{2n} l_i \sin \tau_i \omega; \quad M_\omega^{y_1} = C_2 - \omega^2;$$

$$C_\omega^{y_1} = \sum_{i=1}^{2n} l_i \cos \tau_i \omega - C_t \sum_{i=1}^{2n} l_i \sin \tau_i \omega; \quad N_\omega^{y_1} = C_1 \omega \quad (10)$$

$$W_{y_2}(i\omega) = \frac{K_\omega^{y_2} + iC_\omega^{y_2}}{J_{rt}(M_\omega^{y_2} + iN_\omega^{y_2})};$$

$$K_\omega^{y_2} = C_t \sum_{i=1}^{2n} l_i \cos \tau_i \omega + \mu_t \omega \sum_{i=1}^{2n} l_i \sin \tau_i \omega; \quad M_\omega^{y_2} = d_2 - \omega^2;$$

$$C_\omega^{y_2} = \sum_{i=1}^{2n} l_i \cos \tau_i \omega - C_t \sum_{i=1}^{2n} l_i \sin \tau_i \omega; \quad N_\omega^{y_2} = d_1 \omega \quad (11)$$

Amplitude frequency characteristics, i.e., vertical  $A_z$ , longitudinal-angle  $A_\varphi$ , and transverse for the front  $A_{y_1}$  and rear  $A_{y_2}$  half-frames, are the corresponding modules of complex values (8)-(11)  $|W_z(i\omega)|$ ,  $|W_\varphi(i\omega)|$ ,  $|W_{y_1}(i\omega)|$ , and  $|W_{y_2}(i\omega)|$ :

$$A_z = \frac{1}{\mu} \sqrt{\frac{(K_\omega^z)^2 + (C_\omega^z)^2}{(M_\omega^z)^2 + (N_\omega^z)^2}}$$

$$A_\varphi = \frac{1}{J_{lt}} \sqrt{\frac{(K_\omega^\varphi)^2 + (C_\omega^\varphi)^2}{(M_\omega^\varphi)^2 + (N_\omega^\varphi)^2}}$$

$$A_{y_1} = \frac{1}{J_{ft}} \sqrt{\frac{(K_\omega^{y_1})^2 + (C_\omega^{y_1})^2}{(M_\omega^{y_1})^2 + (N_\omega^{y_1})^2}}$$

$$A_{y_2} = \frac{1}{J_{rt}} \sqrt{\frac{(K_\omega^{y_2})^2 + (C_\omega^{y_2})^2}{(M_\omega^{y_2})^2 + (N_\omega^{y_2})^2}} \quad (12)$$

The Fourier transform of the microroughness correlation function in the longitudinal and transverse planes of the trail allows obtaining the spectral density or energy spectrum  $S(\omega)$  of a random process, which describes the frequency composition of the correlation function.

The correlation functions  $\sigma$  determine the dispersion and mean square deviations (MSD) of the corresponding oscillations:

$$\sigma_z^2 = \frac{1}{\pi} \int_0^\infty S(\omega) A_z^2 d\omega$$

$$\sigma_\varphi^2 = \frac{1}{\pi} \int_0^\infty S(\omega) A_\varphi^2 d\omega$$

$$\sigma_{y_1}^2 = \frac{1}{\pi} \int_0^\infty S(\omega) A_{y_1}^2 d\omega$$

$$\sigma_{y_2}^2 = \frac{1}{\pi} \int_0^\infty S(\omega) A_{y_2}^2 d\omega \quad (13)$$

Mean square deviations  $\sigma_z$ ,  $\sigma_\varphi$ ,  $\sigma_{y_1}$  and  $\sigma_{y_2}$  characterize the spread of values for vibration amplitudes relative to their grouping centers. These are mathematical expectations  $m_z$ ,  $m_\varphi$ ,  $m_{y_1}$ , and  $m_{y_2}$ , which correspond to the quiescent state, i.e., conditions of static load [20].

When studying the dynamic motion of a wheel and probability of suspension breakdown, the linear dependence of these parameters on the statistical characteristics of vertical and longitudinal angular oscillations of a body occurs, namely, on the value of casual square deviations. It allows concluding that the definition of the dynamism coefficient  $k_d$  depends on the energy spectra of oscillations and values corresponding to  $\sigma_z$ ,  $\sigma_\varphi$ ,  $\sigma_{y_1}$  and  $\sigma_{y_2}$ .

Considering these characteristics as dimensional when  $\sigma_z$  has a metric dimension and the rest are angular, it is required to analyze the possibility of their dimensionless representation, in particular, by correlating them to their processes at the quiescent state, i.e., to their mathematical expectations (scale

of measurement). The obtained dimensionless mean square deviations  $\bar{\sigma}_Z$ ,  $\bar{\sigma}_\varphi$ ,  $\bar{\sigma}_{\gamma_1}$ , and  $\bar{\sigma}_{\gamma_2}$  characterize the degree of dynamic amplification (compared to the static) of the oscillating system in vertical, longitudinal angular, and transverse planes.

**Semi-suspended way of skidding.**

The scheme of transverse angular ( $\gamma$ ) oscillations of the tractor weight and bundle suspension ( $\beta$ ) is shown in Fig. 4a considering the roll that occurs when hitting the microroughness of the harmonic profile. Differential equations of oscillations can be presented as:

$$c_1 y + c_1 \beta + c_1 \dot{y} = f_1(t - \tau_1) \quad (14)$$

$$d_1 \dot{y} + d_1 \beta + d_1 \ddot{y} = 0 \quad (15)$$

where  $c_1 = \frac{J_t + G(D+L)^2}{9g}$ ,  $c_2 = \frac{DG(1+L)}{9g}$ ,  $c_3 = \frac{1}{2} c_t n d^2 - GH_k - \frac{2}{3} GL$ ,  $d_1 = c_2$ ,  $d_2 = \frac{QD^2}{9g}$ ,  $d_3 = \frac{2}{3} QD$ ,  $J_t$  is the moment of inertia in the transverse plane relative to the axis of the roll;  $Q$  is the weight of a bundle;  $D$  is the distance from the point of suspension to the point of the bundle center;  $L$  is the distance from the center of the roll to the point of suspension;  $G$  is the weight of the tractor;  $Nk$  is the distance from the point of tractor's mass center to the base of its front half-frame;  $Jnk$  is the moment of inertia of the bundle with respect to the axis passing through the point of suspension and the touch center of the second end of the bundle with soil;  $fI(t-\tau_i)$  is the function of action considering the lag time  $\tau_i$ . It is believed that tractor has  $\frac{2}{3}Q$ .

By multiplying both parts of the equations (14) and (15) by  $e^{-St}$  and integrating within the range from 0 to  $\infty$ , we obtain the Laplace transform leading the system of differential equations to a system of algebraic equations relative to the new complex variable  $S$ :

$$(c_1 S^2 + c_3) y(S) + c_2 S^2 \beta(S) = F_1(S) \quad (16)$$

$$d_1 S^2 y(S) + d_2 S^2 + d_3 \beta(S) = 0 \quad (17)$$

After solving the system of equations (16)-(17) and taking  $S=i\omega$ , where  $\omega$  is the frequency of forced vibrations,  $1/s$  result in amplitude frequency characteristics of transverse vibrations of the tractor and the timber bundle:

$$W_y(i\omega) = \frac{d_3 - d_3 \omega^2}{(c_3 - c_1 \omega^2)(d_3 - d_3 \omega^2) - d_1^2 \omega^4};$$

$$W_\beta(i\omega) = \frac{d_1 \omega^2}{(c_3 - c_1 \omega^2)(d_3 - d_2 \omega^2) - d_1 \omega^4} \quad (18)$$

The scheme of vertical and longitudinal angular oscillations is accepted as a scheme with a flexible rod, in which an element with length  $Ls$  (a pack of logs with the weight  $Q$ ) is connected to the weight of tractor  $M$ , and the technological module is  $\frac{2}{3}Q$  (Fig. 4a).

The end of the rod lying on the ground is considered pinched. Thus, at point  $A$

we have the mass  $M_a = M + \frac{2}{3}Q$ , which performs

vertical ( $Z$ ) and longitudinal ( $\varphi$ ) oscillations, described by two differential equations (rigidity of the rod at bending is neglected):

$$M_a Z + 2n\mu Z + 2n\dot{Z} + M_a l_1 \varphi + 2n\mu l_1 \varphi + 2nc\varphi = 2n(\mu q + c_t q) \quad (19)$$

$$M_a (l_1^2 + p_y^2) \varphi + 2n\mu l_1^2 \varphi + 2ncl_1^2 \varphi + 2M_a l_1 Z + 2M_a l_1 \dot{Z} + 2ncl_1 Z = 2n(\mu_t l_1 q + c_t l_1 q)$$

where  $\rho_y$  is inertia radius of  $M_a$  mass in longitudinal plane;  $n$  is the number of axes.

Representing equations (19) in the operator form and having performed necessary Laplace and Fourier transformations considering relations, the amplitude frequency characteristics of vertical  $W_z$

( $i\omega$ ), longitudinal angular  $W_\varphi$  ( $i\omega$ ), and transverse oscillations of a tractor are obtained:

$$W_z(i\omega) = \frac{i\mu_1 \omega - c_t}{\frac{M_a \omega^2}{4} - \mu_t i \omega - c_t}$$

$$W_\varphi(i\omega) = \frac{1}{2M_a p_y^2 (\frac{M_a \omega^2}{4} - 2\omega^3 \mu_t i - 2c_t \omega)} \quad (20)$$

Based on the principles of the stationary random functions theory, the spectral densities of the amplitudes of the corresponding oscillations are determined by multiplying the squares of the modules of quantities (18) and (20) by the spectral density  $S(\omega)$  of profile microroughness.

Thus, the energy spectra of the oscillations will form:

- In vertical plane –  $S_z(\omega) = [W_z(i\omega)^2]S(\omega)$
- In longitudinal plane –  $S_\varphi(\omega) = [W_\varphi(i\omega)^2]S(\omega)$  (21)
- Transversely to the tractor –  $S_y(\omega) = [W_y(i\omega)^2]S(\omega)$
- Transversely to the bundle –  $S_\beta(\omega) = [W_\beta(i\omega)^2]S(\omega)$

**Semi-suspended skidding**

This scheme (Fig. 4b) has several differences in comparison with the semi-suspended method scheme [16]. First, the bundle forms a single system with the tractor half-frames, and the bundle roll angle is  $\beta=0$ , i.e., the system roll is considered by the angle  $\gamma$ . The technological module has  $\frac{2}{3}Q$ , and the trail  $\frac{1}{3}Q$ .

The differential equations of vertical ( $Z$ ) and longitudinal ( $\varphi$ ) oscillations are similar to equations (19). The differences occur in the implementation of transverse oscillations, and it is noteworthy to distinguish the transverse oscillations of the front ( $\gamma_1$ ) and rear ( $\gamma_2$ ) halves:

$$y_1 + c_1 y_1 + c_2 y_1 = \frac{1}{J_{ft}} (\sum_{i=1}^{2n} \mu_t l_i y_i + \sum_{i=1}^{2n} c_t l_i y_i) \quad (22)$$

$$y_2 + d_1 y_2 + d_2 y_2 = \frac{1}{J_{rt}} (\sum_{i=1}^{2n} \mu_t l_i y_i + \sum_{i=1}^{2n} c_t l_i y_i) \quad (23)$$

where  $c_1 = \frac{\mu_t}{J_t \left[ \sum_{i=1}^{2n} l_i^2 + \frac{1}{2} d^2 \right]}$ ,  $c_2 = \frac{c_t}{J_{ft}} \left[ \sum_{i=1}^{2n} l_i^2 + \frac{1}{2} d^2 \right]$ ,  $d_1 = \frac{\mu_t}{J_{rt}} \left[ \sum_{i=1}^{2n} l_i^2 + \frac{1}{2} d^2 \right]$ ,  $d_2 = \frac{c_t}{J_{rt}} \left[ \sum_{i=1}^{2n} l_i^2 + \frac{1}{2} p_{x3}^2 n - \frac{H_n G H_3}{c_t} \right]$ ,

$\rho_{xv}$ ,  $\rho_{x3}$  is inertia radii of the front and rear half-frames,  $J_{ft}$  и  $J_{rt}$  their moments of inertia in the transverse plane;  $H_n$  and  $H_3$  are distances from the mass center of the bundle to the half-frame bases.

Then, after the necessary transformations similar to the half-suspended scheme of skidding, transfer functions and amplitude frequency characteristics of vertical  $W_z(i\omega)$ , longitudinal angular  $W_\varphi(i\omega)$ , and transverse oscillations of the front and rear  $W_{\varphi 2}(i\omega)$  half-frames were obtained:

$$W_Z(iz) = \frac{i\mu_t - c_t}{\frac{M_a \omega^4}{4} - \mu_t i \omega - c_t} \quad (24)$$

$$W_\varphi(iz) = \frac{1}{2M_a p_3^2 \left( \frac{M_a \omega^4}{2} - 2\omega^3 \mu_t i - 2c_t \omega^2 \right)} \quad (25)$$

$$W_{y1}(i\omega) = \frac{[c_t \sum_{i=1}^{2n} l_i \cos \tau_i \omega + \mu_t \omega \sum_{i=1}^{2n} l_i \sin \tau_i \omega] + i[\mu_t \omega \sum_{i=1}^{2n} l_i \cos \tau_i \omega + c_t \sum_{i=1}^{2n} l_i \sin \tau_i \omega]}{J_{rt}[(\bar{c}_2 - \omega^2) + i\bar{c}_1 \omega]} \quad (26)$$

$$W_{y2}(i\omega) = \frac{[c_t \sum_{i=1}^{2n} l_i \cos \tau_i \omega + \mu_t \omega \sum_{i=1}^{2n} l_i \sin \tau_i \omega] + i[\mu_t \omega \sum_{i=1}^{2n} l_i \cos \tau_i \omega + c_t \sum_{i=1}^{2n} l_i \sin \tau_i \omega]}{J_{rt}[(\bar{d}_2 - \omega) + i\bar{d}_1 \omega]} \quad (27)$$

The energy spectra of oscillations are determined through the squares of the modules (24)-(27) and the spectral density  $S(\omega)$  of microroughness similarly to equations (21).

### Second subsystem

The second subsystem assumes the elastic soil deformation under dynamic influence arising from the skidding tractor with a bundle of wood.

To assess the condition of the soil under the dynamic influence of the skidding system vibrations, it is relevant to apply the theory of linear elastic and viscous deformation, which is considered to be one of the first rheological theories assuming the common manifestation of elastic and viscous properties of the body. The modeling is based on the Kelvin-Voigt body model [21] with the addition of one elastic element. This model is sometimes called the Hohenzleer-Prager model [22].

The analysis of existing physical-mechanical and mathematical models of elastic and viscous soil condition has shown that the dynamic pressure  $q_d$  exerted by the forwarder on the soil from the dynamic vibrations of the tractor or skidding system can be estimated based on the transfer of acoustic stiffness from one medium to another [23]. Then the pressure transfer coefficient  $k_\lambda$  will be:

$$k_\lambda = \frac{2}{1 + \lambda_1 / \lambda_2} \quad (28)$$

where  $\lambda_1$  is the acoustic stiffness of the wheel lug equal to  $1.1 \cdot 1200 \text{ t/m}^2\text{s}$  and  $\lambda_2$  is the acoustic stiffness of the soil equal to  $0.85 \cdot 800 \text{ t/m}^2\text{s}$ . Thus, the acoustic refraction coefficient  $k_\lambda = 0.68$ .

The acoustic stiffness of the wheel is determined as follows:

$$\lambda_1 = p_t v \quad (29)$$

where  $p_t$  is the density of the tire material,  $\text{kg/m}^3$  and  $v$  is the longitudinal wave speed,  $\text{m/s}$ .

The acoustic stiffness of the soil is determined as follows:

$$\lambda_2 = p v \quad (30)$$

where  $p$  is the density of the soil,  $\text{kg/m}^3$ .

By considering the processes of viscous-plastic soil compaction under the influence of dynamic loads, it is noteworthy that deformations  $\varepsilon$  will not occur instantly but during a finite period [22]. Reconstructing the structure of the medium structure referred to as repacking in the mechanics of soils is a complex internal and intercrystallite processes of "relaying" grains [23]. At comprising a model of dynamic compressibility, it is assumed that there are two diagrams of loading (Fig. 6) - dynamic 1 and static 2.

The compression of spring 1 corresponds to the dynamic diagram, and the total compression of both springs within the proposed model corresponds to the static diagram. The medium is unloaded according to other laws, and the shock compression behind the stress wave surface can cause both the continuous growth or decrease of the stress. In the first case, the deformation and, thus, compaction of the soil will increase due to additional compression of the medium and repacking of the soil grains. In the second case, both the deformation decrease due to unloading and its growth during repacking occur simultaneously. The deformation of  $\varepsilon_d$  corresponds to the dynamic compressibility, while  $\varepsilon_s$  corresponds to the static one, i.e., the deformation of a medium element is defined as the sum of  $\varepsilon = \varepsilon_d + \varepsilon_s$ . Relative soil compaction  $\bar{\rho} = p/p_0$ , where  $p_0$  is initial density, relates to the deformation  $\varepsilon$  by the following ratio [32]:

$$\bar{\rho} = \varepsilon + 1 = \varepsilon_d + \varepsilon_s + 1. \quad (31)$$

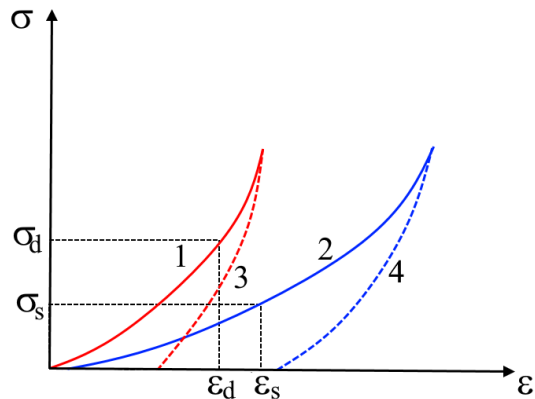


Fig. 6. Loading scheme of viscous-plastic soil: dynamic compressibility (1) static compressibility (2), dynamic unloading (3), and static unloading (4).

Thus, due to the linear nature of the relative density and strain ratio, the compaction value is accepted as the sum of the dynamic and static compaction values. Under shock compression, the

soil deformation of  $\varepsilon$  is determined only by the dynamic compression curve since the deformation of  $\varepsilon_s$  does not occur.

Linear nature of loading dependences is accepted in the first approximation as follows:

$$\sigma_d = E_d \varepsilon_d, \quad \sigma_s = E_s \varepsilon_s, \quad (32)$$

where  $E_d$  и  $E_s$  are dynamic and static deformation modules, respectively.

Neglecting the effect of unloading, the value of the relative dynamic soil compaction can be determined as:

$$\bar{\rho}_d = \frac{\sigma_d}{E_d} + 1. \quad (33)$$

Each passage of the skidding system is accompanied by additional dynamic soil compaction, the maximum value of which depends on the properties of the soil and skidding system, as well as the presence of resonant zones in the frequency spectrum.

Thus, mathematical modeling allows estimating the impact of forest machinery on soil compaction at known weights. Nevertheless, the presented model does not take into account such parameters as moisture and soil type. For example, in work [29], the results of studies on 8x8 tractor demonstrated that not only the level of machine load but also the soil moisture affects the depth of the wheel track. In other studies, the type of soil and its moisture is reported to be of high importance for predicting the influence extent of forest operations [30, 31]. These statements will contribute to further research and complement the presented mathematical model considering the categories and moisture.

#### 4. CONCLUSIONS

Based on the results of this work, the following conclusions are drawn. For theoretical research of the second subsystem "tractor - timber bundle - soil", the methods of statistical dynamics with the presentation of microroughness of the trail surface as a random process or random function were applied to evaluate the dynamic compaction of the soil by a tractor or skidding system. In the study of the soil compaction by skidding tractor and skidding system and considering its dynamic influence, the dynamic system "tractor - wood bundle-soil" was accepted to divide into two subsystems. The first one reflects the vibrations of sprung mass on elastic tires in a radial direction, and the second one represents elastic and viscous soil deformation under the dynamic influence of the oscillating system.

In the first subsystem, it is sufficient to measure the vertical vibrations and vibrations of sprung mass in the longitudinal and transverse planes for studying the dynamic soil compaction by a tractor and a bundle of wood. It was shown that the first subsystem can be considered as a linear oscillating system with constant dynamic parameters. Mathematical modeling of second subsystem was

based on the Kelvin-Voigt model with the addition of one elastic element.

The theory of linear elastic and viscous soil deformation under dynamic influence from vibrations of the skidding system was used to assess the soil condition. This theory is considered as the basis for the rheological theory that considers the common manifestation of elastic and viscous properties of the body.

#### ACKNOWLEDGEMENTS

The work was carried out within the confines of the scientific school "Advances in lumber industry and forestry".

#### REFERENCES

1. Najafi A, Solgi A, Sadeghi SH. Soil disturbance following four wheel rubber skidder logging on the steep trail in the north mountainous forest of Iran. *Soil and Tillage Research*. 2009; 103(1): 165-169. <https://doi.org/10.1016/j.still.2008.10.003>
2. Iraj B, Samira Bahram K, Mehdi A, Farhad, K. Effect of compaction on physical and micromorphological properties of forest soils. *American Journal of Plant Sciences*. 2012; 3(1): 16629. <https://doi.org/10.4236/ajps.2012.31018>
3. Cambi M, Certini G, Neri F, Marchi E. The impact of heavy traffic on forest soils: A review. *Forest ecology and management*. 2015; 338: 124-138. <https://doi.org/10.1016/j.foreco.2014.11.022>
4. Smith D. Computer Simulation of Tractor Ride for Design Evaluation. SAE Technical Paper. 1977; 770704. <https://doi.org/10.4271/770704>
5. Li X, Lv W, Zhang W, Zhao H. Research on dynamic behaviors of wheel loaders with different layout of hydropneumatic suspension. *Journal of Vibroengineering*. 2017; 19(7): 5388-5404. <https://doi.org/10.21595/jve.2017.18277>
6. Pytka JA. Dynamics of wheel-soil systems: a soil stress and deformation-based approach. CRC Press. 2012.
7. Manukovskii AY, Grigorev IV, Ivanov VA, Gasparyan GD, Lapshina ML, Makarova JA, Chetverikova IV, Yakovlev KA, Afonichev DN, Kunickaya OK. Increasing the logging road efficiency by reducing the intensity of rutting: Mathematical modeling. *Journal of mechanical engineering research and developments*. 2018; 41(2): 35-41.
8. El-Sayegh Z, El-Gindy M, Johansson I, Öijer F. Truck tyre-terrain interaction modelling and testing: literature survey. *International Journal of Vehicle Systems Modelling and Testing*. 2017; 12(3-4): 163-216. <https://doi.org/10.1504/IJVSMT.2017.089972>
9. Tullberg, J. *Agricultural Machinery: Problems and Potential*. Research in Agriculture and Applied Economics. 2009; No. 655-2016-44585. <https://doi.org/10.22004/ag.econ.125191>
10. Macdonald P, Clow M. What a difference a skidder makes: The role of technology in the origins of the industrialization of tree harvesting systems. *History and technology*. 2003; 19(2): 127-149. <https://doi.org/10.1080/07341510304139>
11. Rudov S, Grigorev I, Kunickaya O, Ivanov N, Kremleva L, Mueller O, Hertz EF, Chemshikova Y,

- Teterevleva E, Knyazev A. Method of variational calculation of influence of the propulsion plants of forestry machines upon the frozen and thawing soil grounds. *International Journal of Advanced Science and Technology*. 2019; 28(9): 179-197.
12. Oden JT, Reddy JN. *Variational methods in theoretical mechanics*. Springer Science & Business Media. 2012.
  13. Rudov SE, Voronova AM, Chemshikova JM, Teterevleva EV, Kruchinin IN, Dondokov YZ, Khaldeeva MN, Burtseva IA, Danilov VV, Grigorev IV. Theoretical Approaches to Logging Trail Network Planning: Increasing Efficiency of Forest Machines and Reducing Their Negative Impact on Soil and Terrain. *Asian Journal of Water, Environment and Pollution*. 2019; 16(4): 61-75. <https://doi.org/10.3233/AJW190049>
  14. Zhuk AY, Hahina AM, Grigorev IV, Ivanov VA, Gasparyan GD, Manukovsky AY, Kunitskaya OA, Danilenko OK, Grigoreva OI. Modelling of indenter pressed into heterogeneous soil. *Journal of Engineering and Applied Sciences*. 2018; 13(8): 6419-6430.
  15. Manukovsky AY, Grigorev IV, Ivanov VA, Gasparyan GD, Lapshina ML, Makarova YA, Chetverikova IV, Yakovlev KA, Afonichev DN, Kunitskaya OA. Increasing the logging road efficiency by reducing the intensity of rutting: mathematical modeling. *Journal of Mechanical Engineering Research and Developments*. 2018; 41(2): 35-41.
  16. Grigorev MF, Grigoreva AI, Grigorev IV, Kunitskaya OA, Stepanova DI, Savvinova MS, Sidorov MN, Tomashevskaya EP, Burtseva IA, Zakharova OI. Experimental findings in forest soil mechanics. *EurAsian Journal of BioSciences*. 2018; 12(2): 277-287.
  17. Rudov S, Shapiro V, Grigorev I, Kunitskaya O, Druzyanova V, Kokieva G, Filatov A, Sleptsova M, Bondarenko A, Radnaed D. Specific features of influence of propulsion plants of the wheel-tyre tractors upon the cryomorphic soils, soils, and soil grounds. *International Journal of Civil Engineering and Technology*. 2019; 10(1): 2052-2071.
  18. Ferguson TS. *A course in large sample theory*. Routledge. 2017.
  19. Shahgoli G, Fielke J, Saunders C, Desbiolles J. Simulation of the dynamic behaviour of a tractor-oscillating subsoiler system. *Biosystems engineering* 2010; 106(2): 147-155. <https://doi.org/10.1016/j.biosystemseng.2010.03.002>
  20. Klubnichkin VE, Klubnichkin EE. Research of kinematics and dynamics of tracked timber harvesting vehicle running gear. In: *Forest engineering: making a positive contribution. Abstracts and Proceedings of the 48th Symposium on Forest Mechanization, Linz, Austria*. 2015. Institute of Forest Engineering, University of Natural Resources and Life Sciences; 2015: 315-320
  21. Bland DR. *The theory of linear viscoelasticity*. Courier Dover Publications. 2016.
  22. Jing Z, Benin D, Snezhko V, Vorona-Slivinskaya I, Aksenov I. Mechanical stresses in building structures and dry friction - ways to improve the durability of architectural structures *Jour of Adv Research in Dynamical & Control Systems*. 2020;12(2): 578-585.
  23. Li X, Gong F, Tao M, Dong L, Du K, Ma C, Zhou Z, Yin T. Failure mechanism and coupled static-dynamic loading theory in deep hard rock mining: a review. *Journal of Rock Mechanics and Geotechnical Engineering*. 2017;9(4):767-782. <https://doi.org/10.1016/j.jrmge.2017.04.004>
  24. Kremers J, Boosten M. Soil compaction and deformation in forest exploitation. *American Journal for Alternative Agriculture*. 2018; 7(1-2), 25-31.
  25. Cambi M, Hoshika Y, Mariotti B, Paoletti E, Picchio R, Venanzi R, Marchi E. Compaction by a forest machine affects soil quality and *Quercus robur* L. seedling performance in an experimental field. *Forest Ecology and Management*. 2017; 384: 406-414. <https://doi.org/10.1016/j.foreco.2016.10.045>
  26. Riggert R, Fleige H, Horn R. An assessment scheme for soil degradation caused by forestry machinery on skid trails in Germany. *Soil Science Society of America Journal*. 2019; 83(s1): S1-S12. <https://doi.org/10.2136/sssaj2018.07.0255>.
  27. Marusiak M, Neruda J. Dynamic soil pressures caused by travelling forest machines. *Croatian Journal of Forest Engineering: Journal for Theory and Application of Forestry Engineering*. 2018; 39(2): 233-245. <https://hrcak.srce.hr/204192>
  28. Bulat PV, Chernyshev MV. Existence regions of shock wave triple configurations. *International Journal of Environmental and Science Education*. 2016; 11(11): 4844-4854.
  29. Uusitalo J, Ala-Ilomäki J, Lindeman H, Toivio J, Siren M. Predicting rut depth induced by an 8-wheeled forwarder in fine-grained boreal forest soils. *Annals of Forest Science*. 2020; 77: 1-10. <https://doi.org/10.1007/s13595-020-00948-y>
  30. Islamutdinov VF Factors affecting the development of the machine-building and metal-working industry in the Khanty-Mansi autonomous Okrug — Yugra. *Economy of Region*. 2018; 14(4):1424-1437
  31. Mohieddinne H, Brasseur B, Spicher F, Gallet-Moron E, Buridant J, Kobaissi A, Horen H. Physical recovery of forest soil after compaction by heavy machines, revealed by penetration resistance over multiple decades. *Forest Ecology and Management*. 2019; 449: 117472.

Received 2020-05-19

Accepted 2020-05-18

Available online 2020-11-09



**Igor GRIGOREV** is a Doctor of Technical Sciences, Professor of the Department of Technology and Equipment of Forest Complex, Yakut State Agricultural Academy, Yakutsk, Russian Federation. Field of research: logging and reforestation machinery, equipment and procedures



**Ol'ga KUNICKAYA** is a Doctor of Technical Sciences, Professor of the Department of Technology and Equipment of Forest Complex, Yakut State Agricultural Academy, Yakutsk, Russian Federation. Field of research: timber production; wood modification; the use of wood as energy;

environmental safety of timber harvesting and processing facilities; wood chemical industry; and utilization of non-timber forest products



**Albert BURGONUTDINOV** is a Doctor of Technical Sciences, Professor of the Department of Roads and Bridges Building, Perm National Research Polytechnic University, Perm, Russian Federation. Field of research: thermal conductivity of building materials in road structures (i.e., monitoring of soil and pavement temperature at 3-m depth); developing guidelines for

traffic circle construction.



**Viktor IVANOV** is a Doctor of Technical Sciences, Vice-Rector of the Bratsk State University, Bratsk, Russian Federation. Field of research: technology and machinery for logging and forestry.



**Svetlana SHUVALOVA** is a Candidate of Pedagogic Sciences, Associate Professor of the Department of Descriptive Geometry and Engineering Graphics, Saint Petersburg State University of Architecture and Civil Engineering, Saint-Petersburg, Russian Federation. Field of research: geometric modeling, problems of higher education pedagogy in the

framework of sustainable development.



**Viktoria SHVETSOVA** is a Candidate of Technical Sciences, Associate Professor of the Department of Descriptive Geometry and Engineering Graphics, Saint-Petersburg State University Architecture and Civil Engineering, Saint-Petersburg, Russian Federation. Field of research: three-dimensional models of hardscape elements.



**Marina STEPANISHCHEVA** is a Doctor of Technical Science, Associate Professor of the Department of Reproduction and Processing of Forest Resources, Bratsk State University, Bratsk, Russian Federation. Field of research: technology and machinery for logging and forestry.



**Evgeniy TIKHONOV** is a Candidate of Technical Sciences, Assistant Professor of the Department of Transport and Technological Machinery and Equipment, Federal State Budget Educational Institution of Higher Education "Petrozavodsk State University", Petrozavodsk,

Russian Federation. Field of research: mechanization of agriculture, industrial aquaculture technologies and equipment, and combined applications of supercooled plasma technology